Verification of a Predictive Formula for Critical Shear Stress with Large Scale Levee Erosion Experiment

Yagisawa, Junji; van Damme, Myron; Pol, J.C.; Bricker, Jeremy

Publication date
2019

Document Version
Accepted author manuscript

Published in
Proceedings of the 11th ICOLD European Club Symposium

Verification of a Predictive Formula for Critical Shear Stress with Large Scale Levee Erosion Experiment

J Yagisawa, PhD.[1], M van Damme, PhD.[2], JC Pol, M.Eng[3], JD Bricker, PhD [4]
1. Assoc. Prof., Saitama University, Saitama, Japan
2. Position, Delft University of Technology, Delft, The Netherlands
3. Position, Delft University of Technology, Delft, The Netherlands
4. Assoc. Prof., Delft University of Technology, Delft, The Netherlands

ABSTRACT

Apart from the soil erodibility parameter, the critical shear stress is the most important parameter in predicting erosion rates. On the basis of experiments several empirical formulas have already been developed which relate the critical shear stress to soil properties. Based on these findings and supported by new large scale experiments, a new predictive relation between the critical shear stress and soil properties is proposed here. In support of this study, Delft University of Technology collaborated with Saitama University in the preparation and execution of a large scale levee erosion experiment in January 2019. The erosion experiments were performed in the on a 1.8m high levee with a sand core and respectively clay and loam cover types. The cover types were subjected to a constant overflow discharge of approximately 70 l/m/s. The test levee was constructed in the Flood Proof Holland test polder in Delft, The Netherlands. During the experiment, time lapse measurements of the erosion depth were obtained at 15 locations along the landside slope. Before and after overflow tests were performed on each cover type, soil samples were collected along the landside slope at 8 locations. This paper outlines how these large experiments were used to evaluate the effectiveness and application limit of the new predictive equation for the critical shear stress. A comparison between the predicted and measured erosion rates shows that by applying the new empirical relation for the critical shear stress, measured erosion rates could be predicted around ±30 % errors.

Keywords: large scale levee erosion experiment, erosion rate, critical shear stress, erodibility

1 INTRODUCTION

Many water management issues, including river channel degradation, bank stability, bridge scour, and levee and earthen dam overtopping, stem from excessive erosion of cohesive soils. Therefore, the ability to accurately predict cohesive soil erosion is a necessity for engineers worldwide. Providing accurate predictions is challenging because of numerous factors influencing soil erodibility such as soil texture, soil moisture condition, compaction, organic matter content, chemical properties, and biological properties (e.g. Knapen et al. (2007); Grabowski et al. (2011)).

Typically, the erosion rate of a cohesive soil is predicted using a model that relates soil erodibility to hydraulic forces on the soil. The stress-based detachment equation, shown in Eq.(1), is widely used in many previous studies for embankment overtopping (Temple et al. (2005)), bank erosion (Simon et al. (2011)), and internal erosion (Wan & Fell (2004)).

$$E_s = k_d \, (\tau - \tau_c)^{\alpha} \quad (1)$$

where E_s : erosion rate (m/s), k_d : erodibility coefficient (m^3/sN), τ : bed shear stress (N/m^2), τ_c : critical shear stress required to initiate detachment for the material (N/m^2), and α : an exponent (generally assumed to be one (e.g. Hanson & Simon (2001)).

Apart from the soil erodibility coefficient, the critical shear stress is the most important parameter in predicting erosion rate. On the basis of experiments several empirical formulas have already been developed which relate the critical shear stress to soil properties.

Smerdon & Beasley (1959), and Julian & Torres (2006) have proposed predictive formulas for critical shear stress based on soil texture and Ockenden & Delo (1988), Mitchener & Torfs (1996), and Amos et al.(2004) have provided predictive formulas for the critical shear stress based on soil density. While some predictive formulas for τ_c have been proposed based on only a single soil property, Hanson & Hunt (2007) clarified the effect of initial soil moisture content, fine fraction content and dry density (compaction degree) on soil erodibility, and they have reported that changes in soil erodibility largely depend on the degree of compaction and water content during compaction even in soil having the same fine fraction content. This indicates that it is difficult to predict τ_c based on only a single soil property. In order to estimate the erosion rate accurately, it is necessary to propose and verify a predictive formula for τ_c considering multiple soil properties.

Therefore the objectives of this study are to: 1) propose a predictive formula for τ_c based on multiple soil properties by using the results of previous studies; 2) verify the accuracy of that formula against a large scale levee erosion experiment; and 3) apply the predictive formula of τ_c in this study and various formulas proposed by previous researchers to the results of Briaud et al. (2008), and confirm how well each formula can predict the observed erosion rate.

2 TEST METHODOLOGY

2.1 *Experimental setup of large scale levee erosion experiment*

Erosion experiments were performed on a 1.8m high levee with a sand core and respectively clay and loam landside slope covers (Fig. 1i, ii, iii). The test levee was constructed in the Flood Proof Holland test polder in Delft, The Netherlands. As shown in Fig.1i, a 1 m wide flume was created for each cover type. Before and after overflow tests were performed on each cover type, soil samples were collected along the landside slope at 8 locations for each flume. For the soil sampling, a steel pipe with 2 cm inner diameter and 30 cm length was used. As shown in Fig. 1ii, soil samples were taken at 3 points from the outside of the flume before overflow and 5 points from the inside of the flume after overflow, respectively. Table 1 shows some soil properties for both cover types.

2.2 *Overflow characteristics*

During the experiment, both sections were subject to a maximum overflow discharge of approximately 70 l/m/s. However, the overflow was generated differently in each case. For the Loam section, water supply to the upstream side of the levee was held constant at approximately 70 l/m/s, while overflow was prevented by a flashboard installed across the flume entrance on the crest of the levee. When the water depth above the levee crest reached 8 cm, the flashboard was quickly removed, and overflow started. However, in the Clay section, water was supplied to the upstream side of the levee at approximately 40 l/m/s in the initial stage of the experiment, and the overflow was initiated. However,

since no

Table 1. Soil properties for Clay and Loam cover types.
For the samples, each character represents C: Clay, L: Loam, 1, 3, 5: distance from top of levee along land side slope (m)

Samples	Bulk density	Dry density	Grain size		Fine fraction content	Water content
	ρ (kg/m^3)	ρ_d (kg/m^3)	%sand >63 μ m	% fines <63 μ m	*FC* (%)	*WC* (%)
C1	1781	1344	33.7	66.3	66.3	27.9
C3	1681	1347	41.2	58.8	58.8	24.8
C5	1719	1370	37.0	63.0	63.0	30.0
L1	1402	1358	59.1	40.9	40.9	20.4
L3	1369	1369	62.9	37.1	37.1	21.9
L5	1358	1402	61.6	38.4	38.4	16.1

erosion occurred during the first 45 minutes of testing at 40 l/m/s test, the overflow discharged was increased to approximately 70 l/m/s by powering on an extra pump. Overflow durations for the Loam section and Clay section were 60 minutes and 130 minutes, respectively.

2.3 *Measurement of overflow discharge and erosion depth*

During overflow, both water depth and flow velocity were measured at the center of the levee crest and at the center of the flume, and the erosion depths were measured along the landside slope (Fig. 1iii). Water depths were measured by fixing rulers to both side walls installed on the top of levee and reading them directly (Fig. 1iv). An electromagnetic current meter was installed at a position approximately half of the water depth above the levee crest, and the flow velocity was measured at a sampling frequency of 100 Hz. From the data, the flow rate per unit width during the experiment was obtained.

The erosion depth was measured at 15 points in total at the positions shown in Fig. 1iii. For the measurement, a pin profiler (Fig. 1v) was used and the difference from the initial ground height was measured by reading from the tape measure attached to the pin profiler. Measurement of water depth and erosion depth were conducted at 5 minute and 2.5 minute intervals in the Clay and Loam sections, respectively.

2.4 *Calculation of Erosion rate*

To confirm the validity of the predictive formula for τ_c, the measured erosion rates ($E_{s\text{-}obs}$) were compared against the calculated erosion rates ($E_{s\text{-}cal}$). $E_{s\text{-}obs}$ was obtained from the measured erosion depths and a total of five $E_{s\text{-}obs}$ values were estimated as the averaged depth for each cross section where pin profiler was set as described in Section 2.3. To obtain $E_{s\text{-}cal}$ (Eq. (1)), it is necessary to estimate k_d and τ in addition to τ_c. The power coefficient a, has thereby been assumed as 1. Therefore, Section 2.4.1 explains the method used to derive τ_c and k_d, and Section 2.4.2 describes the numerical simulation for τ. Note that the deposition rate was assumed to be zero for the purpose of this analysis.

2.4.1 *Predictive formulas for τ_c and k_d*

As mentioned in the introduction, many predictive formulas for τ_c have been proposed previously, but most of them account for only one soil property. However, as pointed out by Hanson & Hunt (2007), τ_c is likely to depend upon not only one soil property but a multitude of soil properties. In order to identify the dependence on the different soil properties, data from previous studies into τ_c have been examined and referenced here. With reference to Hanson & Hunt (2007), three typical soil properties were selected: fine fraction content (*FC* (%)), dry density (ρ_d (kg/m^3)) and soil moisture content (*WC* (%)). As shown in Table 2, 48 data sets were acquired from four previous studies. By performing multiple regression analysis using these data, a predictive formula for τ_c was obtained as follows,

$$\tau_c = -91.77 + 0.289FC + 0.062\rho_d - 0.035WC \qquad (2)$$

Fig. 2 shows the comparison between the observed τ_c and the value calculated using Eq. (2). The coefficient of determination R^2 of this equation (Eq. (2)) is 0.78. Regarding the soil erodibility k_d, Hanson & Simon (2001) and Simon et al. (2011) measured a correlation with τ_c, and they proposed equations (3) and (4), respectively.

$$k_d = 0.0002\tau_c - 0.5 \qquad (3)$$

$$k_d = 0.0016\tau_c\text{-}0.84 \quad (4)$$

In our study, Equation 4 (Simon et al., 2011) was used to calculate k_d (Eq. (4), with additional experimental data added to Eq. (3) (Hanson & Simon (2001)).

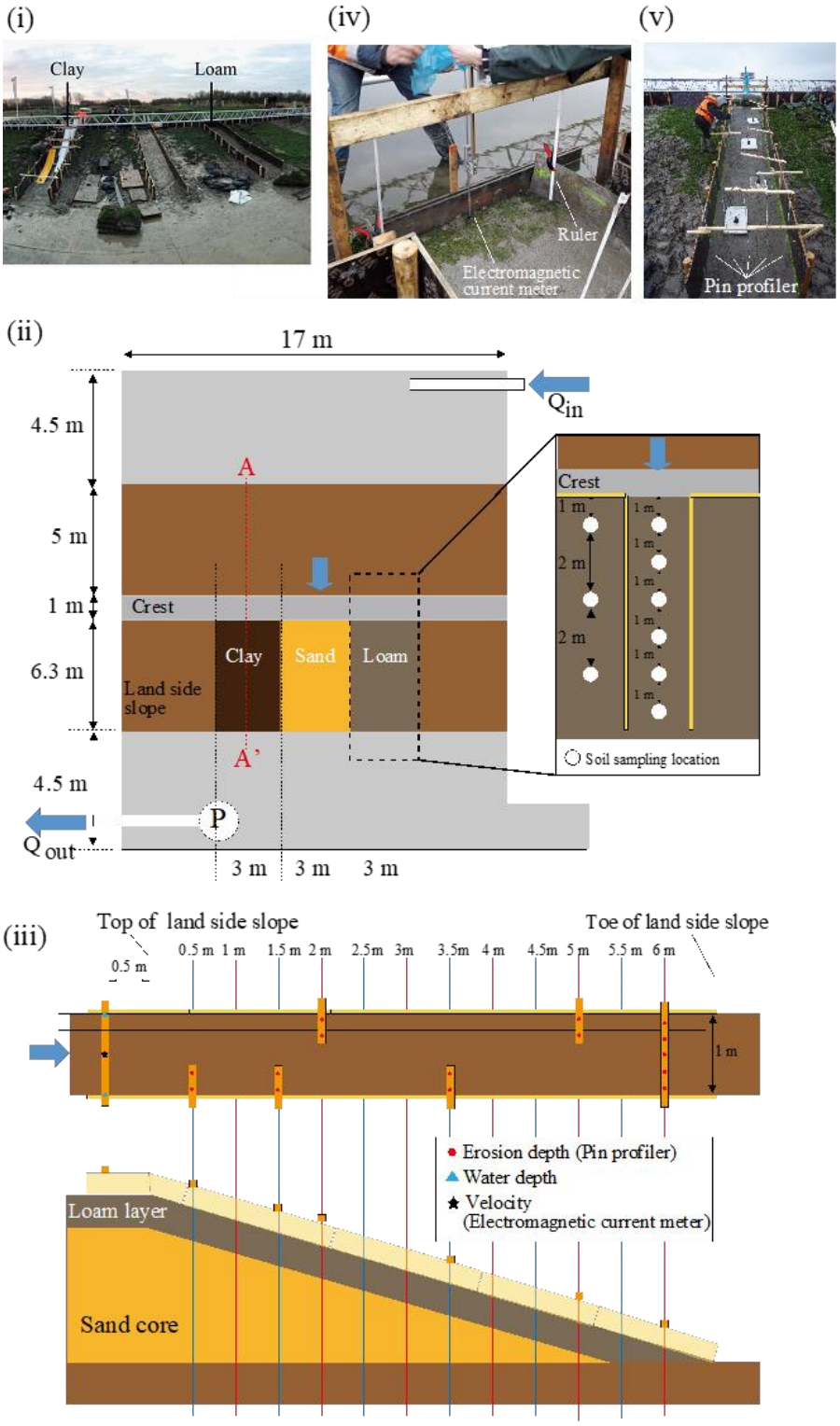

Figure 1. Experimental set up.
(i) overview of test levee, (ii) plain view of test polder, (iii) top view of channel and side view of test levee, with measurement locations for erosion depth, (iv) water depth and velocity measurement at levee crest, (v) set up of pin profiler for measuring erosion depth

2.4.2 *Predictive formulas for τ_c and k_d*

The shear stress τ necessary for calculation of $E_{s\text{-}cal}$ was obtained by using the CADMUS-SURF two-dimensional vertical (2DV) single-phase Volume of Fluid (VOF) flow model. CADMUS-SURF has been validated for overflow of a steeply sloping surface (e.g. Hanzawa et al. (2012)). Simulation of our experiments is computationally expensive, so as shown in Fig.3, a total of 6 cases (four time intervals (T1 to T4) for the Clay case and two time intervals (T1 to T2) for the Loam) case were chosen for simulation. The following two points are the reasons for choosing these time intervals. 1: This flow model does not consider bed elevation change during overflow. Therefore, T1 and T2 were selected to

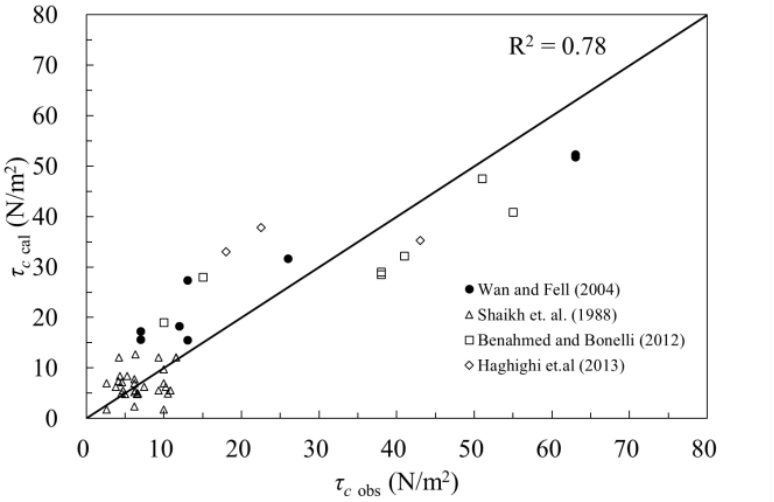

Figure 2. The observed critical shear stress ($\tau_{c\text{-}obs}$) in previous studies vs. predicted critical shear stress ($\tau_{c\text{-}cal}$) using Eq. (2).

Table 2. The range of soil physical properties of the previous studies utilized for the derivation of Eq. (2).

References	Num. of data	Critical shear stress τ_c (N/m^2)	Fine fraction content SC (%)	Dry density ρ_d (kg/m^3)	Water content WC (%)
Shaikih et al. (1988)	30	2.59 - 11.59	40 - 100	1110 -1420	22.5 - 41.0
Wan and Fell (2004)	8	7 - 63	20 - 84	1585 - 1968	15.2 - 21.2
Benahmed and Bonelli (2012)	7	10 - 55	30 - 95	1500 - 1920	15 - 24
Haghighi et al. (2013)	3	18 - 43	65 - 100	1600 - 1800	19 - 26

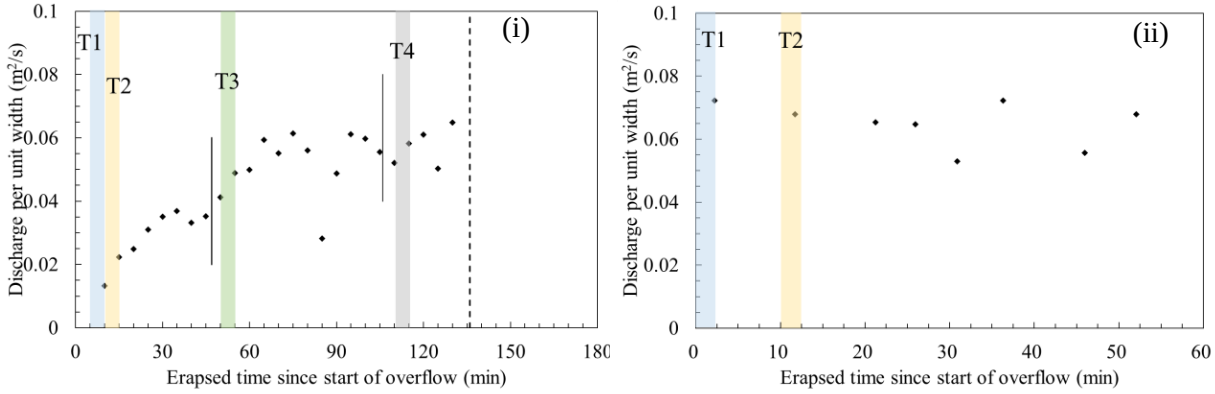

Figure 3. Time series of discharge per unit width and time intervals for numerical simulation of shear
stress, τ in each case (i) Clay case, (ii) Loam case

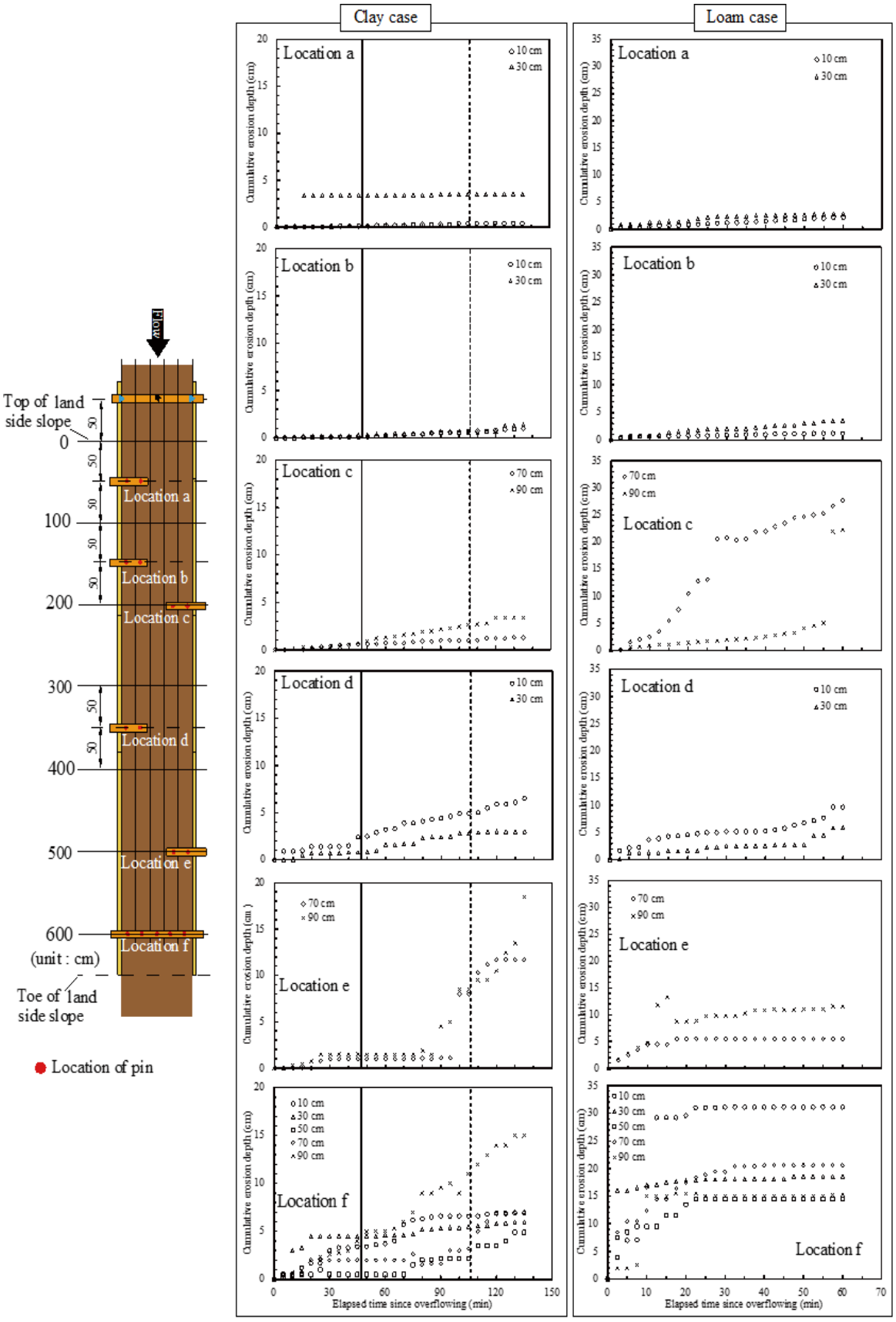

Figure 4. Time lapse of erosion depth along land side slope in each case
The numbers in each legend indicate the transverse distance from the right side wall. Vertical lines indicate when flowrate was stepped up by activating extra pumps for the Clay case.

understand the relationship between τ and $E_{s\text{-}obs}$ in a state still near the initial topography, and 2: since T3 and T4 are set about 1-2 hours after the onset of overflow, it is assumed that erosion has progressed greatly by these time. T3 and T4 were also selected in order to obtain the erosion rate under various conditions of bed level and τ.

In this calculation, flow rate per unit width at each time interval was specified as the inflow to the reservoir. Each numerical simulation was performed for 120 seconds (sufficient for development of steady flow) with a grid size in the horizontal direction Δx = 2 cm, grid size in the vertical direction Δz = 0.5 cm, and time step of $\Delta t = 1\times10^{-4}$ sec.

3 RESULTS

3.1 *Time lapse of erosion depth*

Fig. 4 shows the time series of erosion depth for both the Clay and Loam cases. Regarding the Clay case, the flow rate is increased by adding pumps after 47 minutes and 106 minutes have elapsed from the start of overflow. These times are indicated by solid and dotted lines, respectively. As a common tendency in both cases, erosion was small at locations a and b on the upper slope, nor did the erosion depth grow rapidly in time. On the other hand, at point f at the slope toe, erosion depth grew rapidly after the start of overflow, and continued to grow throughout the experiment. Comparing the Clay and Loam cases, the erosion depth in the Clay case is smaller at any given elapsed time. The fraction content *FC* of the Clay and Loam cases in this experiment were about 60 % and 40 % respectively (Table 1). As reported by many previous researchers (e.g. Julian & Torres (2008); Gilley et al. (1993)), the same tendency was shown that τ_c was larger in soil with greater *FC*.

3.2 *Comparison between $E_{s\text{-}obs}$ and $E_{s\text{-}cal}$*

Fig. 5 shows a comparison of $E_{s\text{-}obs}$ and $E_{s\text{-}cal}$ calculated using the predictive formula for τ_c (Eq.(2)). In this figure, a line of perfect fit and lines of ± 30% error are shown. In both the Clay and Loam cases, it can be seen that many data points fall within ± 30% error. However, $E_{s\text{-}cal}$ is considerably underestimated in comparison with $E_{s\text{-}obs}$ at locations e and f (red circles in Fig. 5) near the toe where particularly large erosion rates were measured. Fig. 6 shows the time lapse of the erosion depth at locations e and f for the Clay case, and the erosion depth contours after the experiment. As can be seen from Fig. 6iii, a gully of depth of about 15 – 20 cm formed along the left side wall around locations e and f. The process in which this gully formed is as follows. First, as shown in Fig. 6ii (location f), a rapid increase in erosion depth occurred 80 minutes after the start of overflow. Ten minutes after that, a sharp increase in erosion depth was observed at location e (Fig. 6i). This indicates that erosion rapidly propagated from downstream (location f) to upstream (location e), due to local formation of a head cut. This type of erosion is accompanied by mass failure, and is difficult to resolve by a formula targeting surface erosion as in Eq. (1).

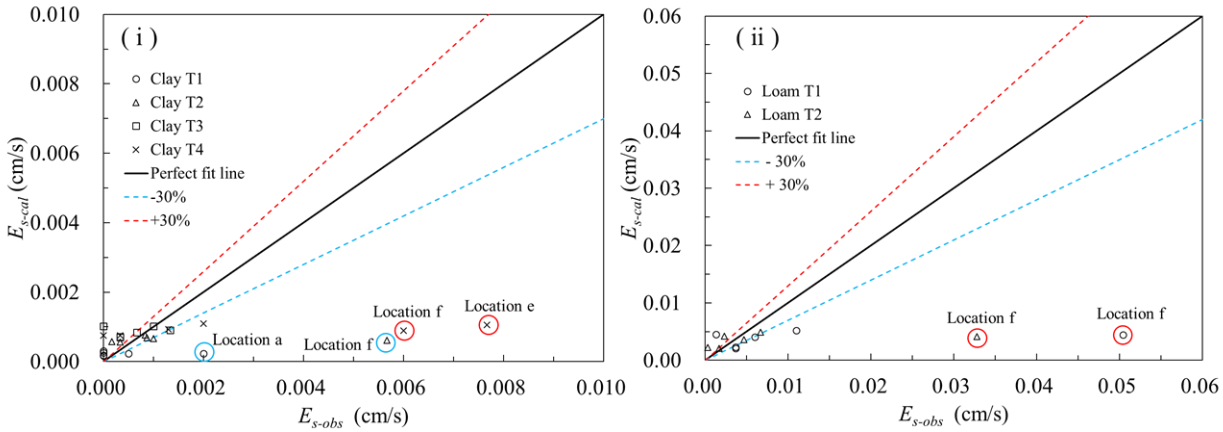

Figure 5. Comparison between observed erosion rate $E_{s\text{-}obs}$ and predicted erosion rate $E_{s\text{-}cal}$
(i) Clay case, (ii) Loam case. Locations a, e, and f shown by red and blue circles correspond to the locations shown in Figure 4.

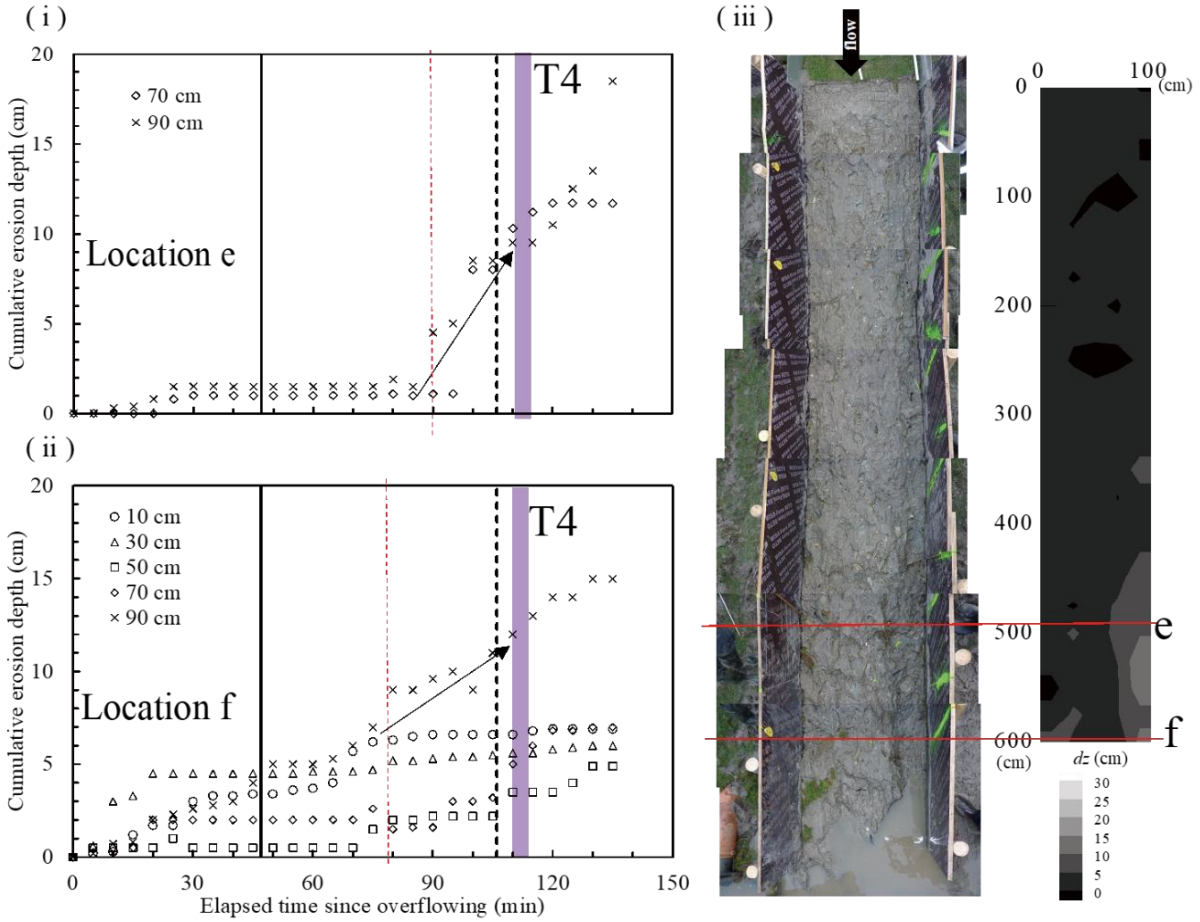

Figure 6. Erosion around locations e and f for Clay.
(i) time lapse of erosion depth at location e, (ii) time lapse of erosion depth at location f, (iii) contour of erosion depth after experiment.

For the Clay case, as indicated by the blue circles in Fig. 5i, erosion depth on the scale of 2-3 cm was measured despite the small flow rate at times T1 and T2. As shown in Figs. 7i and ii, no significant erosion occurred after erosion of 2-3 cm at these locations. Since erosion is accomplished by head-cutting as described above, erosion does not proceed uniformly in time. This is illustrated by a small soil block that suddenly and locally detached from the levee surface as shown in Fig. 7iii. On the other hand, in the Clay case (Fig. 5i), it was confirmed that $E_{s\text{-}cal}$ was large even though $E_{s\text{-}obs}$ was 0. The cause of this may be the influence of large local erosion (such as gully formation) on the left bank side (Fig. 6iii). In fact, the flow concentrates where erosion is large, and the shear stress decreases at the measurement point for erosion depth near the right sidewall. However, since the numerical simulation used in this study does not consider topography changes, calculated shear stress is expected to be greater than actual one. Except for the above points, it was confirmed that the erosion rate can be predicted with 38% relative error by using the formula for τ_c (Eq. (2)). In addition, despite the limitations mentioned above, it was confirmed that Eq. (2) can estimate the order of magnitude of the erosion rate.

4 DISCUSSION

4.1 *Comparison of predictive formulas for τ_c proposed in previous studies to experimental results by Briaud et al. (2008)*

In this section, we apply the predictive formula of τ_c in this study (Eq. (2)) and various formulas proposed by previous researchers to the results of Briaud et al. (2008), and confirm whether each formula can evaluate observed erosion rate. Briaud et al. (2008) evaluated erosion rate using an Erosion

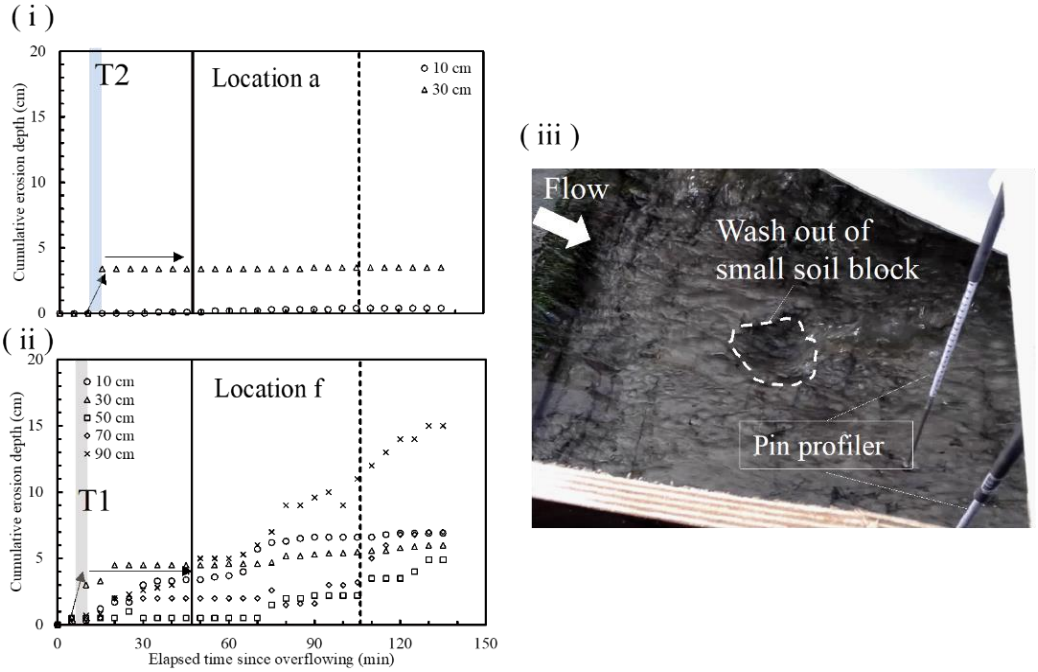

Figure 7. Erosion around points a and f for Clay.
(i) time lapse of erosion depth at point a, (ii) time lapse of erosion depth at point f, (iii) wash out of small soil block

Table 3. Experimental range of soil physical properties of Briaud et al. (2008) and the applicable range of each predictive formula for τ_c.

References	Related soil physical property for predicting τ_c	Fine fraction content SC (%)	Dry density ρ_d (kg/m^3)	Water content WC (%)	Shear stress τ (N/m^2)
Briaud et al. (2008)	-	67.2 - 97.3	1264 - 1700	16.1 - 38.9	0.3 - 110.0
Eq. (w) in this article	SC, ρ_d, WC	20 - 100	1110 - 1968	15 - 41	0.1 - 153.5
Julian and Torres (2006)	SC	5 - 95	n.a	n.a	n.a
Smerdon and Beasly (1959)	SC	15 - 57	n.a	n.a	1.0 - 4.2
Ockenden and Delo (1988)	ρ_d	34 - 100	50 - 1400	n.a	0.14 - 0.41

n.a : not available

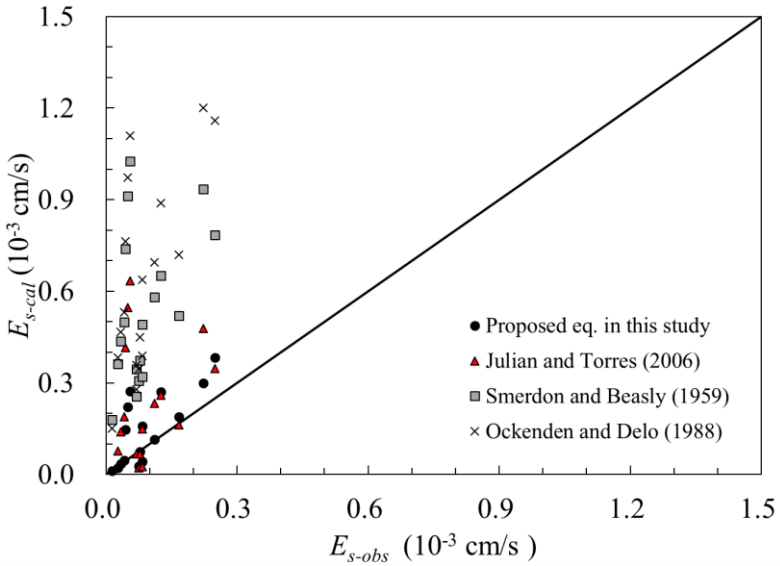

Figure 8. Comparison of the $E_{s\text{-}obs}$ by Briaud et al. (2008) with $E_{s\text{-}cal}$ calculated from each predictive formula.

Function Apparatus (EFA) for soil collected from coastal levees damaged by Hurricane Katrina in 2005. Two previous studies that predicted τ_c based on *FC* are Julian & Torres (2006) (Eq. (5)) and Smerdon & Beasly (1959) (Eq.(6)), while Ockenden & Delo (1988) (Eq. (7)) related the critical shear stress to ρ_d.

$$\tau_c = 0.1 + 0.1779FC + 0.0028FC^2 - 2.34\times10^{-5} FC^3 \quad (5)$$

$$\tau_c = 0.493\times10^{0.0182FC} \quad (6)$$

$$\tau_c = 0.0013\rho_d^{1.2} \quad (7)$$

Although many previous researchers pointed out that WC also greatly affects erodibility (e.g. Gilley et al. (1993)), a predictive formula for τ_c with *WC* as a variable was not found within the extent of our review. Table 3 shows the experimental range of soil physical properties and applied shear stress of Briaud et al. (2008) and each predictive formula for τ_c. Fig. 8 shows a comparison of $E_{s\text{-}obs}$ of Briaud et al. (2008) with $E_{s\text{-}cal}$ calculated from each predictive formula.

In the case of Smerdon & Beasly (1959) which based the predictive formula on *FC*, $E_{s\text{-}cal}$ was 3.1 to 18.5 as large as $E_{s\text{-}obs}$. In the case of Julian & Torres (2006), which based the predictive formula on *FC* as well, $E_{s\text{-}cal}$ is 0.3 to 11.4 times as large as $E_{s\text{-}obs}$, a smaller error than Smerdon & Beasly (1959). The reason for this is that the range of *FC* applicable to each predictive formula. Julian & Torres (2006) used *FC* up to 95 %, while Smerdon & Beasly (1959) used materials with high sand content and *FC* of up to only 57 %. In the case of Ockenden & Delo (1988) which constitutes the only predictive formula with ρ_d, the resulting $E_{s\text{-}cal}$ is 4.0 – 20.0 times $E_{s\text{-}obs}$. Possibly this predictive formula is based on soil with low values for ρ_d. In our new predictive formula, there are several points of overestimation, but the range of error is only 0.4 – 4.9 times $E_{s\text{-}obs}$. The predictive formula for τ_c proposed in this article shows a predictive accuracy of erosion rate higher than other formulas which each consider a single soil physical property, especially for the lower range of erosion rates. Hanson & Hunt (2007) investigated the effect of degree of compaction and soil moisture content on erodibility. According to their results, erodibility changes greatly depending on the compaction degree (related to soil density) and moisture content even in soil with the same *FC*.

4.2 *Validity of the predictive formula of* k_d *in Simon et al. (2011)*

In this study, Eq. (4), proposed by Simon et al. (2011), was used for predicting k_d. In order to confirm the validity of this formula, a regression equation was obtained using experimental data of several previous works as shown in Fig. 9. This further testifies to the validity of Simon et al. (2011), with an R^2=0.52. The contradicts Knapen et al. (2007), which summarized 151 field experiments and 179 laboratory experiments and reported that there was no correlation between between τ_c and k_d, as their da-

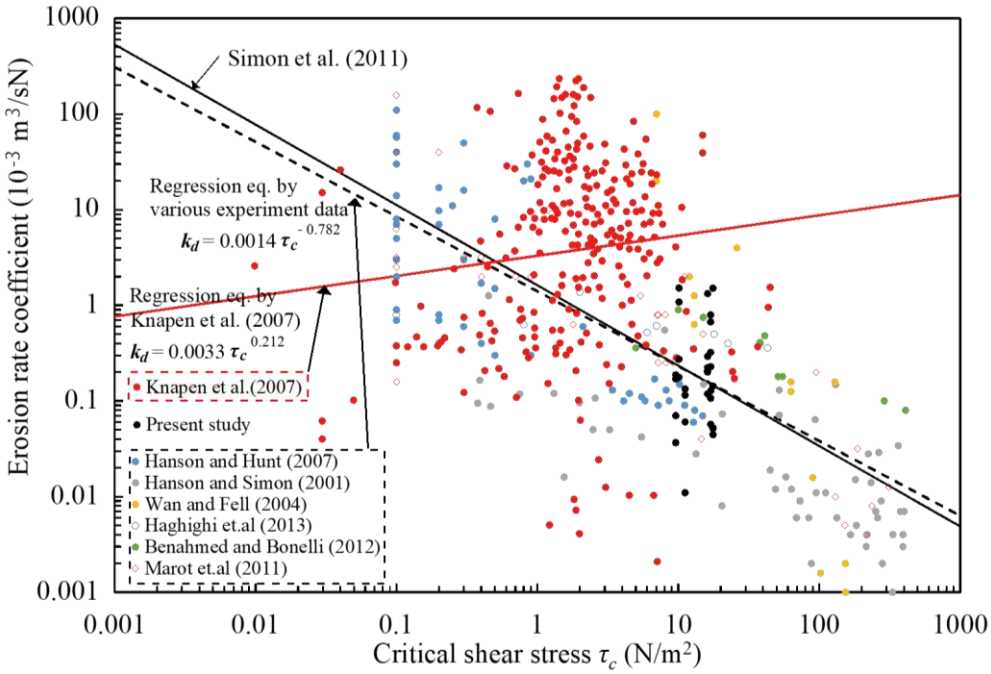

Figure 9. Relationship between τ_c and k_d in previous works and regression equations for k_d.

ta
alone showed a regression correlation coefficient R^2 of only 0.01. Even though Knapen et al. (2007) investigated a large volume of previous research data, this data was focused on field experiments from croplands. In such field conditions, it is expected that the surface soil has a low degree of compaction and low dry density. Conversely, Simon et al. (2011) used data of τ_c and k_d obtained only from in-situ and laboratory jet erosion tests of the soil from flood plains and riverbanks. The data that we added to Fig. 9 are also limited to laboratory flume and jet erosion tests results. Although the values of compaction degree are not specified in these experimental data, their compaction degree is expected to be considerably higher than that of cropland soil. Wan & Fell (2004) also pointed out that compaction degree is one of the main soil properties affecting erodibility. In order to predict k_d with high accuracy, it appears essential to consider the degree of compaction of surface soil in flood defences.

In Fig. 9, the data obtained from our experiments were also plotted (filled black circles). The k_d values of these points are calculated from the Eq. (1) based on the measured erosion rate. It can be seen that these data points fall quite close to the predictive formula for k_d proposed by Simon et al. (2011). Therefore, it seems reasonable to apply their predictive formula for k_d to our experiment.

5 CONCLUSIONS

The conclusions obtained in this study are shown below.

1) A comparison between the predicted and measured erosion rates obtained by a large scale levee ersion test shows that by applying a new empirical relation for the critical shear stress (Eq. (2)), measured erosion rates could be predicted with 38% relative error. However, it also confirmed that this formula cannot be applied to erosion caused by head-cutting mass failure.
2) As a result of comparing measured erosion rates from Briaud et al. (2008) with erosion rates predicted by the new formula proposed in this study and several previous studies, we found that more accurate prediction is achieved by using the new empirical relation incorporating multiple physical soil properties.

ACKNOWLEDGEMNET

This work was supported by JSPS KAKENHI Grant Number 17H04936. TU Delft is grateful for funding by the Netherlands Organization for Scientific Research (NWO) TTW grant 13861 (SAFELevee) and Cooperation China NWO/NSFC/EPSRC Joint Research Projects Sustainable Deltas grant ALWSD.2016.007 (Shanghai Flood Risk). The authors would like to thank Z. Li, L. Lian and P. Van der Gaag for their help with respect to levee erosion test.

REFERENCES

Amos, C.L., Bergamasco, A., Umigiesser, G., Cappucci, S., Cloutier, D., DeNat, L., Flindt, M., Bonardi, M., Cristante, S., 2004. The Stability of tidal flats in Venice Lagoon – the results of in-situ measurements using two bentic, annular flumes. Journal of Marine Systems 51, 211-241.

Benahmed, N., Bonelli, S., 2012. Internal erosion of cohesive soils: laboratory parametric study, 6th International Conference on Scour and Erosion, 8p.

Briaud, J.L., Chen, H.C., Govindasamy, A.V., Storesund, R., 2008. Levee erosion by overtopping in New Orleans during the Katrina Hurricane, Journal of geotechnical and geoenvionmental engineering, ASCE, 134(5), 618-632.

Gilley, J.E., Elliot, W.J., Laflen, J.M., Simanton, S.R., 1993. Critical shear stress and critical flow rates for initiation of rilling, Journal of Hydrology 142, 251–271.

Grabowski, R.C., Droppo, I.G., Wharton, G., 2011. Erodibility of cohesive sediment: The importance of sediment properties, Earth-Science Reviews 105, 101-120.

Haghighi, I., Chevalier, C., Duc, M., Guedon, S., Reiffsteck, P., 2013. Improvement of hole erosion test and results on reference soils, Journal of Geotechnical and Geoenvironmental Engineering 139(2), 330-339.

Hanson, G.J., Hunt, S.L., 2007. Lessons learned using laboratory JET method to measure soil erodibility of compacted soils, Applied Engineering in Agriculture 23(3), 305-312.
Hanson, G.J., Simon, A., 2001. Erodibility of cohesive streambeds in the loess area of the Midwestern USA, Journal of Hydrological Processes 15(1), 23-38.
Hanzawa, M., Matsumoto, A., Tanaka, H., 2012. Applicability of CADMAS-SURF to evaluate detached breakwater effect on solitary tsunami wave reduction, Earth Planets Space 64, 955-964.
Julian, J.P., Torres R., 2006. Hydraulic erosion of cohesive riverbanks. Geomorphology 76, 193-206.
Knapen, A., Poesen, J., Govers, G. Gyssels, Nachtergaele, J., 2007. Resistance of soils to concentrated flow erosion: A review, Earth-Science Reviews 80, 75-109.
Marot, D., Regazzoni, P.L., Wahl, T., 2011, Energy-based method for providing soil surface erodibility rankings, Journal of Geotechnical and Geoenvironmental Engineering 137(12), 1290-1293.
Mitchener, H., Torfs, H., 1996. Erosion of mud / sand mixtures, Coastal Engineering 29, 1-25.
Ockenden, M.C., Delo, E.A., 1988. Consolidation and erosion of estuarine mud and sand mixtures: An experimental study, Hydraulics Research Wallingford 49.
Simon, A., Pollen-Bankhead, N., Thomas, R.E., 2011. Stream Restoration in Dynamic Fluvial Systems: Scientific Approaches, Analyses, and Tools, Geophysical Monograph Series 194, 453-474
Smerdon, E.T., Beasley, R.P., 1959. The tractive force theory applied to stability of open channels in cohesive soils, University of Missouri College of Agriculture Research bulletin 715, 1-36.
Temple, D.M., Hanson, G.J., Neilson, M.L., Cook, K.R. 2005. Simplified breach analysis model for homogeneous embankments: Part 1, Background and model components. In Proc. 25th Annual United States Society on Dams (USSD). Denver, Colo.: USSD.
Wan, C.F. Fell, R., 2004. Investigation of rate of erosion of soils in embankment dams. J. of Geotech nical and Geoenvironmental Engineering, ASCE 130(4), 373-380.